



Preliminary assessment of the effectiveness of neoadjuvant chemotherapy in breast cancer with the use of ultrasound image quality indexes

Anna Pawłowska^a, Norbert Żołek^{a,*}, Beata Leśniak-Plewińska^b, Katarzyna Dobruch-Sobczak^{a,c}, Ziemowit Klimonda^a, Hanna Piotrkowska-Wróblewska^a, Jerzy Litniewski^a

^a Institute of Fundamental Technological Research, Polish Academy of Sciences, Warsaw, Poland

^b Warsaw University of Technology, Department of Mechatronics, Warsaw, Poland

^c The Maria Skłodowska-Curie Institute - Oncology Center, Warsaw, Poland

ARTICLE INFO

Keywords:

Quantitative ultrasound
Image quality
Neoadjuvant chemotherapy
Breast cancer
Treatment response

ABSTRACT

Objective: Neoadjuvant chemotherapy (NAC) in breast cancer requires non-invasive methods of monitoring its effects after each dose of drug therapy. The aim is to isolate responding and non-responding tumors prior to surgery in order to increase patient safety and select the optimal medical follow-up.

Methods: A new method of monitoring NAC therapy has been proposed. The method is based on image quality indexes (IQI) calculated from ultrasound data obtained from breast tumors and surrounding tissue. Four different tissue regions from the preliminary set of 38 tumors and three data pre-processing techniques are considered. Postoperative histopathology results were used as a benchmark in evaluating the effectiveness of the IQI classification.

Results: Out of ten parameters considered, the best results were obtained for the Gray Relational Coefficient. Responding and non-responding tumors were predicted after the first dose of NAC with an area under the receiver operating characteristics curve of 0.88 and 0.75, respectively. When considering subsequent doses of NAC, other IQI parameters also proved usefulness in evaluating NAC therapy.

Conclusions: The image quality parameters derived from the ultrasound data are well suited for assessing the effects of NAC therapy, in particular on breast tumors.

1. Introduction

The use of neoadjuvant chemotherapy (NAC) for breast cancer treatment continuously increases [1–3]. In the case of locally advanced breast cancers and Stage 2 or 3, HER-2 positive or triple-negative breast cancers [4–6], it is a standard procedure preceding radical mastectomy and radiation therapy. The purpose of NAC is to reduce tumor mass, recurrence, and the risk of metastases and micrometastases [7,8]. However, NAC therapy is not successful in every case, the meta-analysis [9] based on the results from 18,000 patients shows the full effectiveness of therapy in only 21.5% of cases. Therefore, monitoring the effects of NAC after each dose of the drug therapy and detecting non-responding tumors as well as detecting, prior to surgery, responding tumors is important as it may influence the choice of further medical procedures. Early isolation of non-responding chemotherapy-resistant tumors avoids unnecessary patient exposure to treatment side effects and may result in a change in the treatment regimen. This is important because over 40% of patients demonstrate a poor pathological response to NAC treatment [10]. Identification of tumors that respond very well

to therapy can increase the percentage of patients treated with breast-conserving therapy, which also significantly affects the psychological condition of the patient [11].

The post-surgical histopathology and assessment of tumor cellularity is a standard approach to determine tumor response to NAC. Current attempts for pre-surgical reliable monitoring of the response to the NAC include MRI, CT, PET, palpation, and ultrasonography [12]. Functional imaging techniques, including PET and MRI, enable imaging of the microstructure and physiology of the tumor [13]. However, the use of these modalities is associated with a high cost, long data collection time, and the need to administer exogenous contrast agents. These factors limit their availability and applicability to monitoring patients during NAC.

Methods that allow non-destructive evaluation of local tissue properties and changes are, if not better, certainly complementary and supportive to methods based on the assessment of changes in tumor size. Quantitative ultrasound (QU) techniques have demonstrated their ability to evaluate tissue structure and its physical properties [14]. This

* Correspondence to: IPPT PAN, ul. Pawinskiego 5B, 02-106 Warszawa, Poland.
E-mail address: nzolek@ippt.pan.pl (N. Żołek).

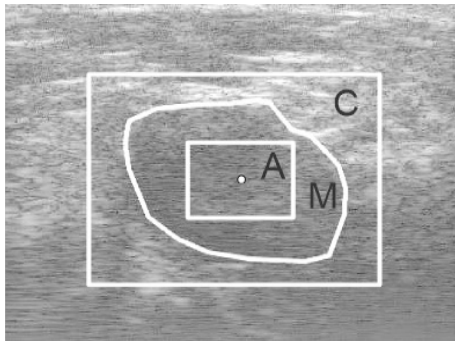


Fig. 1. Areas for which IQI parameters were determined, superimposed on the B-mode image of the lesion. *A* — the rectangular area inside the lesion, *M* — corresponds exactly to the shape of the lesion outlined by the radiologist, *C* — the rectangular area containing the tumor and surrounding tissue, $B = C - A$ — the area near the lesion border.

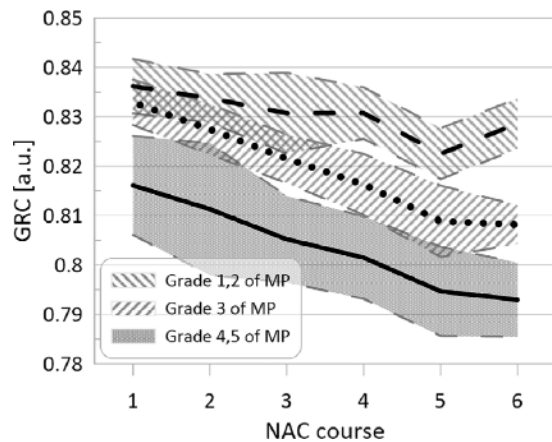


Fig. 2. The mean values of the *GRC* parameter (LOG, C, 22.5%) together with the standard deviation, calculated after consecutive NAC cycles for three groups of tumors. Group of unresponsive tumors (grades 1–2 of MP) — dashed line, grade 3 of MP (dotted line) and responding tumors (grades 4–5 of MP) — solid line.

non-invasive technique has been used to aid in the ultrasound diagnosis of tumors and to monitor neoadjuvant chemotherapy in breast cancer.

The QU methods were applied for monitoring the responsiveness of human breast cancer xenografts in mice [3] using spectral features calculated from RF data and allowed for the prediction of response after the first course of NAC. The classification method based on the integrated backscattering coefficient and the homodyned K distribution shape parameter [15] gave an area under the receiver operating characteristics curve (AUROC), for the shape parameter, equal to 0.69 after the first week of the chemotherapy. The other QU parameters (mid-band fit, spectral slope) were used to determine QU parametric maps. From each map, texture features (such as contrast, correlation, homogeneity, and energy) were evaluated. The homogeneity extracted from the spectral slope map distinguished responding and non-responding patients with an accuracy of 0.79 [16]. The deep learning models were also used to monitor the response to NAC. Siamese convolutional neural network was proposed to calculate the neural features of the lesions. Additionally, the morphological features were determined from tumor images. After the first course of NAC, the neural, morphological, and neural plus morphological methods achieved the AUROC values of 0.826, 0.792, and 0.827, respectively [17].

It needs to be noted that the published results of studies on the monitoring of NAC therapy by ultrasound concern a limited number and types of tumors due to difficulties in collecting data, which is slow, laborious and dependent on the changing condition of the patient.

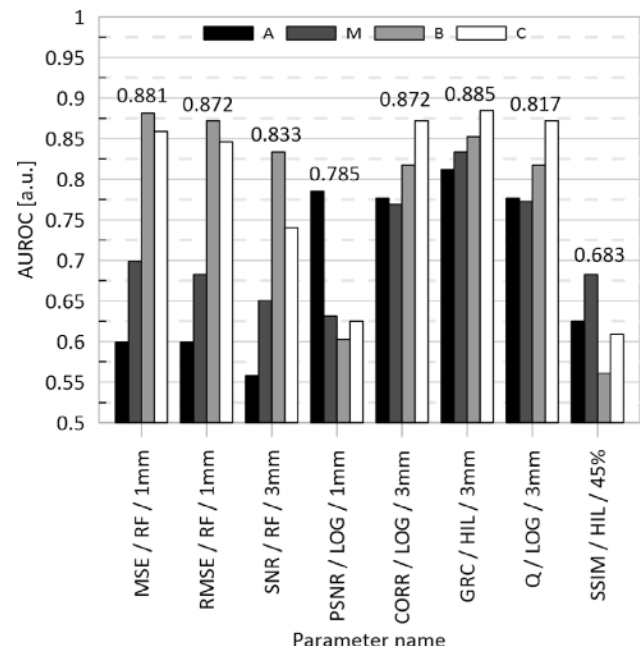


Fig. 3. Determining responding cases. AUROC values evaluating classification models based on each of the eight parameters considered, applied after the first dose of NAC. The color of the bar identifies the area of tissue from which the ultrasound data was collected. Area *A* — the rectangular area inside the lesion, *M* — corresponds exactly to the shape of the lesion outlined by the radiologist, *C* — the rectangular area containing the tumor and surrounding tissue, $B = C - A$ — the area near the lesion border as depicted in Fig. 1.

Table 1

The highest AUROC values after the first NAC cycle along with the standard error, and sensitivity and specificity for detecting responders.

Parameter (Region, Window size, Type)	AUROC [a.u.]	Std. error [a.u.]	Sensitivity	Specificity
<i>GRC</i> (C, 3 mm, HIL)	0.885	0.063	0.833	0.923
<i>CORR</i> (C, 3 mm, LOG)	0.872	0.061	0.833	0.692
<i>Q</i> (C, 3 mm, LOG)	0.872	0.061	0.833	0.692
<i>RMSE</i> (B, 1 mm, HIL)	0.859	0.083	0.833	0.846

Therefore, each new, effective parameter is valuable, increases the reliability of quantitative ultrasound methods, and can be used in a multi-parameter model, potentially increasing the effectiveness of monitoring.

In this work, parameters calculated from ultrasound data are evaluated for monitoring NAC therapy. They are based on the classic Image Quality Indexes (IQI). For example, the grey relational coefficient – *GRC* – parameter has previously been used to compare computed tomography images after compression [18] and ultrasound images of fatty liver [19]. Here, it is applied to ultrasound data from breast tumors and its ability to evaluate the results of NAC therapy is assessed and achieves results at least as good as more complex methods in the literature.

2. Materials and methods

2.1. Data collection

The ultrasound data used for analysis were collected from 29 patients with 38 tumors (two trifocal lesions, five bifocal lesions, twenty-two monofocal lesions). AT (doxorubicin, docetaxel), AC (doxorubicin, cyclophosphamide), and paclitaxel were used in the neoadjuvant treatment. The age of patients ranged from 32 to 83 years (mean 57, median 55, standard deviation 14). The study was approved by the Maria

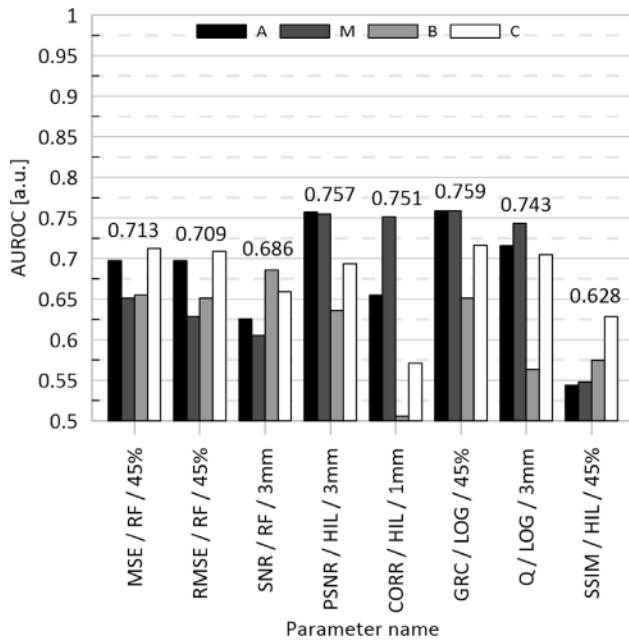


Fig. 4. Determining non-responding cases. AUROC values evaluating classification models based on each of the eight parameters considered, applied after the first dose of NAC. The color of the bar identifies the area of tissue from which the ultrasound data was collected. Area *A* — the rectangular area inside the lesion, *M* — corresponds exactly to the shape of the lesion outlined by the radiologist, *C* — the rectangular area containing the tumor and surrounding tissue, *B* = *C* - *A* — the area near the lesion border as depicted in Fig. 1.

Skłodowska-Curie Memorial Cancer Centre and Institute of Oncology in Warsaw, Poland. All patients signed an informed consent form for participation in the study.

Before NAC, all patients underwent a core needle biopsy for the assessment of histologic grade in breast cancer and the determination of molecular subtype by immunohistochemical markers. All examined tumors type were non-specific (NST). Six (of 38) tumors were luminal A, nine were luminal B HER2+, nine were luminal B HER2-, five were TNBC, and nine were HER2+. All tumor samples were evaluated by the same pathologist.

Raw RF echoes and B-mode images were acquired using an Ultrasonix SonixTouch scanner (formerly Ultrasonix Medical Corporation, Richmond, BC, Canada) with an L14-5/38 linear array transducer (a 128-element transducer with 0.3 mm element pitch, 0.02 mm kerf and 70% fractional bandwidth, excited by two cycles signal of frequency equal to 10 MHz). Each scan consisted of 512 signal lines (filling the 38 mm width of the transducer) recorded at the sampling frequency of 40 MHz. That resulted in about 3376 samples per line. The transducer's focus was always positioned in the middle of the lesion. All examinations were performed by the same radiologist who followed the American College of Radiology BI-RADS guidelines [20]. Each lesion was scanned at various cross-sections to obtain four slices of the region of interest (radial, radial + 45°, anti-radial, anti-radial + 45°). The longest diameter of the tumor was measured. The collected data had the tumor area detected, described and outlined by a radiologist after each ultrasound measurement.

The chemotherapy was followed by mastectomy with lymphadenectomy. In order to categorize the tumor's pathological response to NAC according to the Miller-Payne (MP) scale [21], residual malignant cells (RMC) were quantified using the samples obtained from the biopsy before treatment and the material collected after the treatment and surgery. According to the histopathological results, the tumors were divided into three groups: the group of MP grades 1–2 where 70%–100% of tumor cells remain after chemotherapy, MP grade 3 where

Table 2

The highest AUROC values after the first NAC cycle along with the standard error, and sensitivity and specificity for detecting nonresponding tumors.

Parameter/Region/ Window size/Type	AUROC [a.u.]	Std. error [a.u.]	Sensitivity	Specificity
GRC (A, 22.5%, LOG)	0.759	0.086	0.889	0.69
PSNR (A, 3 mm, HIL)	0.757	0.081	0.889	0.667
CORR (M, 1 mm, HIL)	0.751	0.086	0.778	0.621
Q (M, 3 mm, LOG)	0.743	0.088	0.778	0.759

Table 3

AUROC values after the first, fifth and sixth NAC cycle along with the standard error, and sensitivity and specificity for detecting responders.

Parameter	NAC course	AUROC [a.u.]	Std. error [a.u.]	Sensitivity	Specificity
GRC	1st	0.696	0.101	0.667	0.731
	5th	0.813	0.088	0.750	0.812
	6th	0.985	0.043	1.000	0.861
RMSE	1st	0.872	0.080	0.833	0.923
	5th	0.852	0.086	0.875	0.750
	6th	0.875	0.091	0.833	0.917

Table 4

AUROC values after the first, second and third NAC cycle along with the standard error, and sensitivity and specificity for detecting nonresponding tumors.

Parameter	NAC course	AUROC [a.u.]	Std. error [a.u.]	Sensitivity	Specificity
GRC	1st	0.716	0.100	0.667	0.828
	2nd	0.718	0.096	0.778	0.538
	3rd	0.831	0.096	0.889	0.778
SNR	1st	0.625	0.097	0.667	0.552
	2nd	0.758	0.082	0.667	0.750
	3rd	0.844	0.082	0.889	0.778

10%–70% of tumor cells remain after chemotherapy, and MP grades 4–5 where only at most 10% of tumor cells remain. In our study, the group of MP grades 4–5 was treated as responding and the group of MP grades 1–2 as non-responding.

2.2. Data analysis

Calculation of quantitative measure of lesion change

Image quality based parameters: the mean square error — *MSE*, and its root — *RMSE*, signal to noise ratio — *SNR*, peak *SNR* — *PSNR* [22], grey relational coefficient — *GRC* [23], correlation based parameters as *CORR*, *Q* [24], structural similarity index — *SSIM* [25] were used as a measure of the difference between two datasets obtained from ultrasound data. In particular, we focused on the *GRC* parameter that is used to compute the correlations of discrete sequences. This is equivalent to finding a correlation coefficient between the pixel values in the two grayscale image windows, if the pixel values have been set to sequences. The *GRC* parameter was computed as (1):

$$GRC = \frac{\Delta_{min} + \Delta_{max}}{\Delta_{0i} + \Delta_{max}}, \quad (1)$$

where

$$\Delta_{0i} = \sqrt{\frac{1}{n} \sum_{k=1}^n [\Delta_{0i}(k)]^2}$$

and *n* - the number of pixels in the image, Δ_{0i} - the matrix of absolute values of the differences between the reference image (pre-NAC data, marked 0) and examined image (data after *i*th course), Δ_{min} and Δ_{max} denote the minimum and the maximum of Δ_{0i} matrix, respectively.

Each parameter was calculated using the reference data taken before NAC and data collected after the respective course of chemotherapy. To make calculations reliable, the geometrical mass center of the outlined

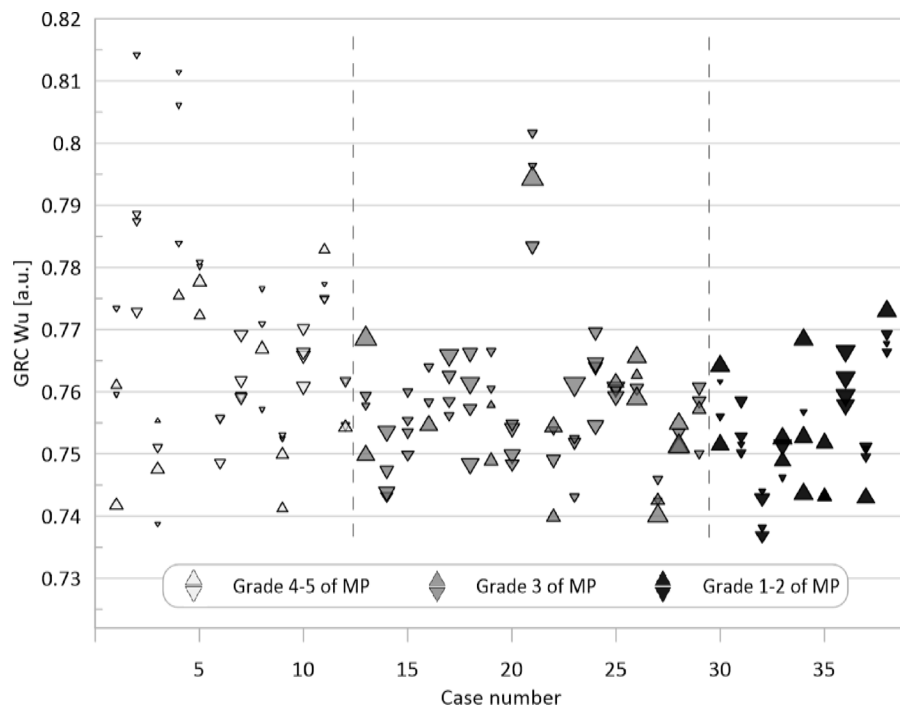


Fig. 5. The values of GRC Wu parameter and change in diameter calculated for all available cases (RF data, region A, averaging window of size 1×1 mm). The size of the point is proportional to the change in diameter (the largest point corresponds to the diameter reduction of 63%). Upward and downward triangles indicate increasing and decreasing change in the maximum diameter of the lesion, respectively. Cases are grouped according to the MP scale. Each case consists of four datasets obtained from different slices.

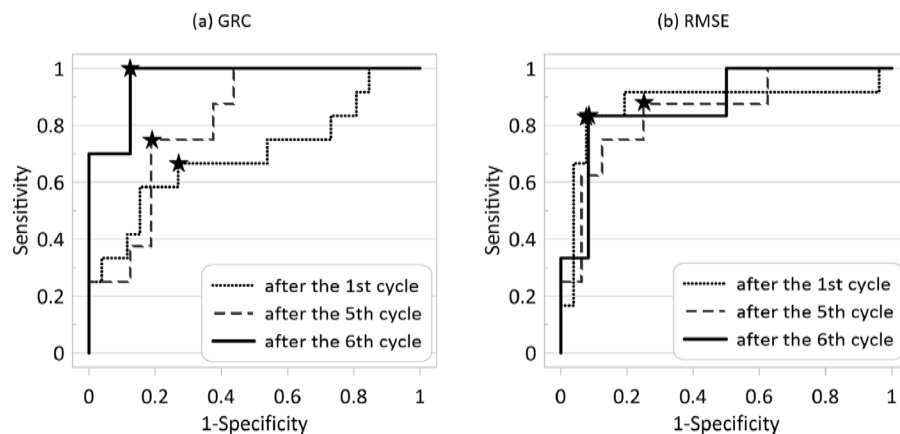


Fig. 6. ROC curves for classification of responding (RMC < 10%) after the 1st, 5th and 6th NAC course. The classifiers are based on GRC (left) and RMSE (right). The markers indicate the operating points for which the parameters are shown in Table 3.

tumor at prechemotherapy measurement was adjusted to the mass center of the lesion after each of the subsequent NAC cycles. Then, four areas of interest around the mass center were defined (Fig. 1). Region A (inside the tumor) was half the horizontal and vertical diameter of the tumor before NAC. The tumor area was designated as the M . Region C was larger than the lesion. It contained the tumor and peritumoral tissue. The dimensions of this rectangular area were equal to the horizontal and vertical diameters of area M multiplied by 1.32. This coefficient was selected to get equality of the area differences between the rectangle C, the rectangle circumscribed on the tumor M , and the rectangle A. Region B was equal to the difference between C and A.

The parameters were calculated in the respective regions using a two-dimensional sliding window. Three types of windows were used, two square ones with a fixed side of 3 mm and 1 mm, and rectangular window with sides depending on the size of the tumor and constituting 22.5% of its horizontal and vertical dimensions.

The size of the 3 mm window was adopted in accordance with [26], where it was shown that it is the size necessary for the proper determination of scattering properties in tissues. On the other hand, the 1 mm dimension ensures adequate tumor coverage [27]. The purpose of the window, the size of which was scaled by the size of the tumor, was to create similar conditions to the analysis of tissue structures dependent on the size of the tumor. In the case of area B, this window was determined based on the thickness of the area. The windows were moved in the analyzed region with a step of one pixel (the window size in pixels was equal to 38×156 [horizontal \times vertical dimension] for the 3 mm \times 3 mm window and 13×52 for 1 mm \times 1 mm, the size in pixels of the window 22.5% varied depending on the tumor size). The value of the IQI parameter was calculated for each window in the examined tissue region. The mean value of the parameter determined for all windows in the region and for four tumor sections was used as a parameter to predict tumor response to NAC.

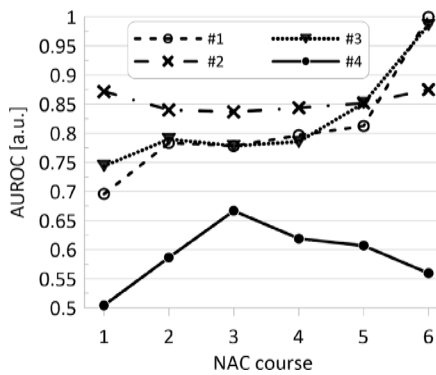


Fig. 7. AUROC values assessing classification models differentiating responding tumors and the remaining group of tumors for subsequent NAC cycles. Parameters shown: #1 *GRC* (HIL, C, 22.5%); #2 *RMSE* (RF, B, 1 mm); #3 *GRC* (HIL, A, 22.5%); #4 Tumor diameter change.

All calculations were applied to the ultrasound raw, post beam-formed data (RF), the Hilbert transform based envelope data (HIL) and log-compressed envelope data (LOG). The RF data contains complete ultrasonic echo information, i.e., amplitude and phase information of the wave backscatter. Envelope data is echo amplitude data often used in quantitative ultrasound to characterize tissues. Log compressed envelope data is very similar to B-mode image data, but is free from the distortion introduced by the signal processing used in ultrasonic scanners for image enhancement. The following notation was used in the description of the IQI characteristics. After the IQI name, in parentheses, we have the data collection area, the type of signal pre-processing and the size of the window used. For example, *GRC* (C, HIL, 3 mm) means that the *GRC* value was determined for the data from the C region, the signal amplitude calculated from the raw data using the Hilbert transform, and the 3 mm \times 3 mm window was applied in the calculations. The Matlab (Mathworks inc.) software was used for the data processing.

Additionally, although Response Evaluation Criteria in Solid Tumors (RECIST) was not originally developed for use in ultrasound data, studies show no difference in the accuracy of RECIST based tumor diameter assessed using MRI and ultrasound data [28]. Therefore, the changes in tumor diameter are also used here to evaluate the effects of NAC.

Statistical analysis

The diagnostic suitability of each parameter as a binary classifier was estimated using ROC analysis. When analyzing the capability of parameters for the differentiation of responders and non-responders, the result of postoperative histopathology (RMC value) was the reference. Two classification models were considered, distinguishing responding from all other patients as well as non-responding from all other patients. The area under the ROC curve (AUROC) with the standard error as well as the sensitivity and specificity were determined. The cutoff value, providing a tradeoff between sensitivity and specificity, was found by maximizing the Youden index [29]. ROC analysis was carried out (using SPSS software, IBM) for the 0.05 significance level.

3. Results

Changes in cancer tissue, caused by successive doses of NAC affect ultrasound scattering, so they should be reflected in IQI values and then may be used to predict the final result of NAC therapy. The mean values of one of the analyzed parameters (*GRC*) during NAC for the three tumor groups, responding (grade 4–5 of MP), non-responding (grade 1–2 of MP) and others (partially responding — grade 3 of MP) are shown in Fig. 2. At each stage of the therapy, the parameter was calculated

using the data from the current NAC cycle and pre-chemotherapy data. The mean value of *GRC* is almost constant after subsequent doses of NAC in the case of tumors non-responding to treatment. On the other hand, for tumors responding to chemotherapy, a monotonic decrease in the *GRC* value is observed.

Since the answer to the question of whether chemotherapy works or not on cancer cells should be obtained as soon as possible, the separability of the responding and non-responding groups of patients after the first chemotherapy was analyzed at the beginning. The curves of receiver operating characteristics (ROC) and the areas under them (AUROC) were determined. The analysis assumed the division of the whole group of tumors into responding (grade 4–5 of MP) and others. The results presented in Fig. 3 show the maximum AUROC values obtained for all parameters considered.

In Table 1, the results obtained for those parameters, after the first NAC dose, AUROC reached the value above 0.85 are presented.

Also when looking for tumors non-responding to NAC, the results (AUROC values from all analyzed windows and data types and tissue areas) obtained after the first dose of the chemotherapy are shown in Fig. 4. The best results were obtained for *GRC*, *Q* and *CORR* and additionally for *PSNR* and the details were summarized in Table 2.

Values of *GRC* parameter calculated for all considered cases after the first course of chemotherapy along with the respective change in diameter of the lesion (depicted as the size of the symbol) are shown in Fig. 5. The parameter's values were obtained for RF data, region A, and averaging window of size 1 \times 1 mm. The different symbol colors indicate the category of Miller–Payne scale to which the case belongs after chemotherapy. The size of the point is proportional to the change in diameter of the respective case (RECIST like index) - the largest change in the considered cases is the diameter reduction of 63%.

The usefulness of image quality indexes for the assessment of NAC was analyzed using data collected from tumors after all subsequent chemotherapy cycles and from all the considered four areas of the tumor. The results presented are showing the greatest ability to reflect tissue changes based on differences in IQI.

In the analysis of the applicability of IQI parameters for the assessment of the effects of NAC in subsequent chemotherapy courses, two parameters, the *GRC* and the *RMSE* are presented. Because the relationship between tissue changes caused by successive chemotherapeutic doses and ultrasound wave scattering, which is the source of changes in IQI parameters, is not fully established, the analysis is focused on results for those IQI parameters that increased or at least maintained the AUROC value during successive chemotherapy cycles.

ROC curves for classification by *GRC* and *RMSE*, selecting tumors responding to NAC therapy, are presented in Fig. 6. In Table 3, AUROC values with standard error and values of sensitivity and specificity calculated for the cut-off points marked on the ROC curves are presented for classification after the first, fifth and sixth NAC cycle.

The results of predicting the positive response of tumors to NAC based on the parameters of *GRC* and *RMSE* in subsequent cycles of chemotherapy are presented in Fig. 7. Additionally, the predictions based on the change in tumor size are included there.

The effectiveness of predicting tumor non-responding to NAC after subsequent treatment cycles was then determined. ROC curves for predicting tumor failure to respond to NAC therapy using *GRC* and *SNR* parameters are shown in Fig. 8.

AUROC values with standard error and values of sensitivity and specificity calculated for the cut-off points marked on the ROC curves (Fig. 8) are presented in Table 4 for classification after the first, second and third NAC cycle.

As in the case of responding tumors, it is assumed that the classification results should not decrease with subsequent treatment cycles. From all considered IQIs, *GRC*, *SNR* and *RMSE* were chosen (Fig. 9). In addition, the classification results based on the size of the tumor are presented.

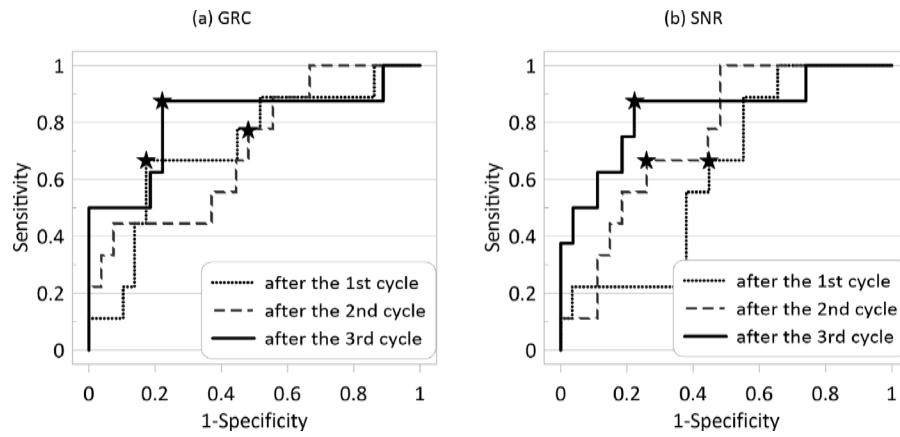


Fig. 8. ROC curves for classification of non-responding tumors (RMC > 70%) after the first 3 NAC courses. The classifiers were based on *GRC* (LOG, *C*, 22.5%) (left), and *SNR* (RF, *M*, 1 mm) (right). The markers indicate the operating points for which the parameters are shown in Table 4.

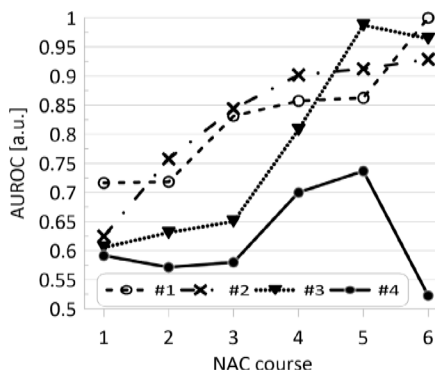


Fig. 9. AUROC values assessing classification models differentiating non-responding tumors and the remaining group of tumors for subsequent NAC cycles. Parameters shown: #1 *GRC* (LOG, *C*, 22.5%); #2 *SNR* (RF, *M*, 1 mm); #3 *RMSE* (RF, *A*, 1 mm); #4 Tumor diameter change.

4. Discussion

For tumors responding to NAC, six IQI parameters achieved AUROC value above 0.8 when calculations were performed on data from *C* or *B* area (Fig. 3). This may suggest that in tumors that respond to NAC, the tissue changes first occur in the outskirts of the tumor. Similarly, the usefulness of ultrasound data from the edge of breast tumors in determining the response of breast cancer to neoadjuvant chemotherapy has been demonstrated in [30]. Also, in differentiating between benign and malignant breast tumors, the importance of ultrasound data from the tissue surrounding the tumor was indicated [31].

The classification using the *GRC* parameter determined for the constant window size (3×3 mm), which worked very well after the first NAC cycle, ranked worse in the subsequent NAC cycles. The *GRC* parameter, calculated for a variable-sized window, classified tumors much better. This may be due to the fact that the window of the size related to the tumor dimensions, indirectly uses information about the tumor size. As a result, treatment-responsive tumors, which are often smaller than non-responsive tumors, also have a smaller averaging window, allowing the detection of small local tissue changes that occur as chemotherapy progresses. As it turns out, this window yields *GRC* parameter values that are more representative of changes in the tumor and its surroundings caused by chemotherapy.

The AUROC value for the *RMSE*-based classification is almost constant throughout the NAC treatment and is about 0.85 (see Fig. 7). Classification based on the *GRC* improves with successive doses of therapy and after the last dose, the corresponding AUROC value approaches

the level close to 1. This applies to the calculations carried out on both data from area *A* and data from area *C*. Since area *A* covers only the central part of the tumor and area *C* the entire tumor, including area *A*, it can be concluded that in this case, the data from the tumor center is the most useful for classification. However, it should be remembered that the reliability of the results obtained from the data collected after the 6th NAC course is lower because the calculations were carried out for a smaller number of cases (18 tumors — NAC therapy was discontinued before the sixth course in some cases). Assessment of the effects of NAC based on changes in tumor dimensions was significantly worse when predicting NAC effects for well-responding tumors.

For tumors non-responding to NAC, the obtained AUROC values are lower than in the case of the tumors responding to NAC. The best results in predicting not responding tumors were obtained with ultrasound data collected from the tumor itself (area *A* and *M* described in Fig. 1), in contrast to tumors that responded well to NAC, for which the area of the peripheral and surrounding tissue was particularly important. In both cases, tumors with good and poor response to NAC, the same parameters (*GRC*, *Q*, and *CORR*) produced the best classification results.

In the case of tumors not responding to NAC, it is important that the information is obtained as soon as possible. The effectiveness of detecting unresponsive tumors increases significantly for all presented IQI parameters with subsequent doses of the drug therapy (Fig. 9). The prognosis of a negative therapy result based on the *GRC* obtained the value of AUROC = 0.84 and 0.86, after courses 3 and 4, respectively, and analogously for the *SNR* parameter, AUROC values = 0.85 and 0.9. Assessment of the effects of chemotherapy on the basis of *RMSE* values was very effective, AUROC = 0.988, but only after the 5th dose of the chemotherapeutic agent. Again, the classification based on tumor diameter was much worse.

The AUROC values obtained in this paper along with State-of-the-art results achieved in the prediction of NAC outcome after the first, second and third course are summarized in Fig. 10. Tumor stiffness as a response marker resulted in AUROC values equal to 0.64 after the 1st cycle [32], 0.75 after the 2nd cycle [32] and 0.73 after the 3rd cycle of NAC [36]. The study [36] also evaluated the discriminative performance of the maximum diameter of the lesion and it allowed to gain accuracy of 0.68. Integrating quantitative contrast-enhanced ultrasound parameters with clinicopathological features increased prediction efficacy from 0.75 to 0.84 [34]. Combined ultrasound and clinicopathological classifiers achieved AUROC of 0.73 at the initial-baseline stage and 0.79 after two cycles of NAC [33]. Neural networks were also used to predict the NAC response. The prediction model based on neural or morphological features resulted in AUROC values ranging from 0.74 to 0.83 [17]. Another developed model using deep learning radiomics achieved an AUROC of 0.81 after the second course

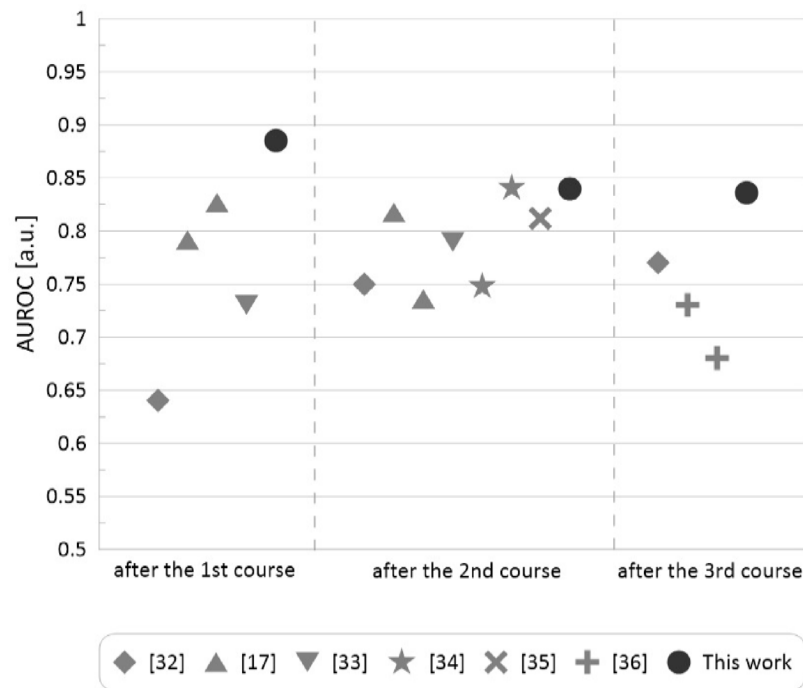


Fig. 10. AUROC values achieved in the prediction of NAC outcome after the first, second and third course in several works [17,32–36] (ordered by publication date). Each symbol shape corresponds to a single published work, multiplied symbols were used to present the results of different approaches. Black circles are the AUROC values obtained in this work.

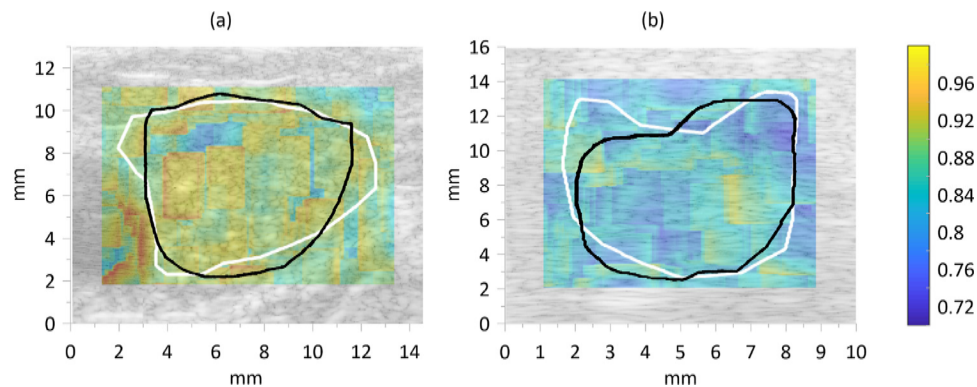


Fig. 11. Parametric images, GRC (HIL, C , 3 mm), of the responding (a) and non-responding (b) breast tumor after the first NAC cycle. The color scale shows the values of the GRC parameter. The lines represent the border of the lesion before chemotherapy (white line) and after the first cycle (black line).

of NAC [35]. Compared to previous studies (AUROC = 0.64–0.84), our method presented the feasibility of predicting NAC outcomes with a higher AUROC value (AUROC = 0.885 after the first stage). The results suggest that the combination of proposed IQI parameters and other modalities features may strongly improve the final result.

The idea of NAC impact assessment using IQI is presented. Parametric maps showing the distribution of GRC parameter values in the tumor after the first chemotherapy for two selected tumor cases, a tumor well responding and a tumor not responding to NAC therapy are presented in Fig. 11. This is the case where none of the tumors change size after chemotherapy, but the GRC values are significantly different. These differences in GRC values illustrate the differences in ultrasound scattering in the tissue of the tumors studied.

5. Conclusions

The results show that IQIs applied for ultrasound data are well suited to assess the effects of NAC therapy. It is particularly important due to the non-invasive nature and low cost of ultrasound diagnostics.

Our research shows that IQI parameters are particularly well suited to predict the effects of NAC on tumors that respond well to therapy. The results obtained show the important role of the tissue surrounding the tumor in predicting a good outcome of NAC therapy. Conversely, for treatment-resistant tumors, a better classification was obtained using data from the tumor itself. The number of analyzed cases is not enough to draw more general conclusions. However, our results indicate that there is great potential to use IQI determined from ultrasound data to observe tissue changes. In the case considered here, these were lesions induced by NAC therapy, but it can be anticipated that also other tissue disease processes, not necessarily related to cancer lesions or chemotherapy, can be detected by the presented method using IQI parameters of ultrasound data.

CRedit authorship contribution statement

Anna Pawłowska: Investigation, Formal analysis, Visualization, Writing – original draft. **Norbert Żółek:** Conceptualization,

Methodology, Investigation, Writing – original draft. **Beata Leśniak-Plewińska**: Validation, Writing – review & editing. **Katarzyna Dobruch-Sobczak**: Data curation. **Ziemowit Klimonda**: Data curation. **Hanna Piotrkowska-Wróblewska**: Data curation. **Jerzy Litniewski**: Supervision.

Declaration of competing interest

The authors declare no conflict of interest.

Data availability

Data will be made available on request.

Acknowledgments

This work was partially supported by grant no. 2019/35/B/ST7/03792 from the National Science Centre of Poland. Special thanks to the Chemotherapy and Radiotherapy Department of the National Cancer Institute in Poland for help in recruiting patients and cooperation.

References

- [1] National comprehensive cancer network (NCCN), in: NCCN Clinical Practice Guidelines in Oncology: Breast Cancer V.1.2019, 2019, <http://www.nccn.org/>.
- [2] X. Feng, et al., Accurate prediction of neoadjuvant chemotherapy pathological complete remission (pCR) for the four sub-types of breast cancer, *IEEE Access* 7 (2019) 134697–134706, <http://dx.doi.org/10.1109/ACCESS.2019.2941543>.
- [3] F. Li, Y. Huang, J. Wang, C. Lin, Q. Li, X. Zheng, Y. Wang, L. Cao, J. Zhou, Early differentiating between the chemotherapy responders and nonresponders: preliminary results with ultrasonic spectrum analysis of the RF time series in preclinical breast cancer models, *Cancer Imaging* 19 (1) (2019) 61–71, <http://dx.doi.org/10.1186/s40644-019-0248-y>.
- [4] C. Morigi, Highlights from the 15th St Gallen international breast cancer conference 15–18 march, 2017, vienna: tailored treatments for patients with early breast cancer, *Ecamermedscience* 11 (732) (2017) <http://dx.doi.org/10.3332/ecancer.2017.732>.
- [5] S.H. Giordano, Update on locally advanced breast cancer, *Oncologist* 8 (6) (2003) 521–530, <http://dx.doi.org/10.1634/theoncologist.8-6-521>.
- [6] K. Dobruch-Sobczak, H. Piotrkowska-Wróblewska, Z. Klimonda, W. Secomski, P. Karwat, E. Markiewicz-Grodzicka, A. Kolańska-Ćwikła, K. Roszkowska-Purska, J. Litniewski, Monitoring the response to neoadjuvant chemotherapy in patients with breast cancer using ultrasound scattering coefficient: A preliminary report, *J. Ultrason.* 19 (77) (2019) 89–97, <http://dx.doi.org/10.15557/JoU.2019.0013>.
- [7] M. Kaufmann, G. von Minckwitz, E. Mamounas, D. Cameron, L. Carey, M. Cristofanili, et al., Recommendations from an international consensus conference on the current status and future of neoadjuvant systemic therapy in primary breast cancer, *Ann. Surg. Oncol.* 19 (5) (2012) 1508–1516, <http://dx.doi.org/10.1245/s10434-011-2108-2>.
- [8] A. Berruti, V. Amoroso, F. Gallo, V. Bertaglia, E. Simoncini, et al., Pathologic complete response as a potential surrogate for the clinical outcome in patients with breast cancer after neoadjuvant therapy: A meta-regression of 29 randomized prospective studies, *J. Clin. Oncol.* 32 (34) (2014) 3883–3891, <http://dx.doi.org/10.1200/jco.2014.55.2836>.
- [9] L. Spring, R. Greenup, K. Reynolds, B. Smith, B. Moy, A. Bardia, Pathological complete response after neoadjuvant chemotherapy predicts improved survival in all major subtypes of breast cancer: systematic review and meta-analyses of over 18, 000 patients, *Cancer Res.* 76 (14) (2016) 1439, <http://dx.doi.org/10.1158/1538-7445.am2016-1439>.
- [10] D. Sethi, R. Sen, S. Parshad, S. Khetarpal, M. Garg, J. Sen, Histopathologic changes following neoadjuvant chemotherapy in locally advanced breast cancer, *Indian J. Cancer* 50 (1) (2013) 58–64, <http://dx.doi.org/10.4103/0019-509X.112301>.
- [11] S.K. Al-Ghazal, L. Fallowfield, R.W. Blamey, Comparison of psychological aspects and patient satisfaction following breast conserving surgery, simple mastectomy and breast reconstruction, *Eur. J. Cancer* 36 (15) (2000) 1938–1943, [http://dx.doi.org/10.1016/S0959-8049\(00\)00197-0](http://dx.doi.org/10.1016/S0959-8049(00)00197-0).
- [12] W.J. Choi, W.K. Kim, H.J. Shin, J.H. Cha, E.Y. Chae, H.H. Kim, Evaluation of the tumor response after neoadjuvant chemotherapy in breast cancer patients: correlation between dynamic contrast-enhanced magnetic resonance imaging and pathologic tumor cellularity, *Clin. Breast Cancer* 18 (1) (2018) e115–e121, <http://dx.doi.org/10.1016/j.clbc.2017.08.003>.
- [13] L. Sannachi, H. Tadayyon, A. Sadeghi-Naini, W. Tran, S. Gandhi, F. Wright, M. Oelze, G. Czarnota, Non-invasive evaluation of breast cancer response to chemotherapy using quantitative ultrasonic backscatter parameters, *Med. Image Anal.* 20 (1) (2015) 224–236, <http://dx.doi.org/10.1016/j.media.2014.11.009>.
- [14] Ruihan Yao, Yufeng Zhang, Keyan Wu, Zhiyao Li, Meng He, Baoping Fengyue, Quantitative assessment for characterization of breast lesion tissues using adaptively decomposed ultrasound RF images, *Biomed. Signal Process. Control* 75 (103559) (2022) <http://dx.doi.org/10.1016/j.bspc.2022.103559>.
- [15] H. Piotrkowska-Wróblewska, K. Dobruch-Sobczak, Z. Klimonda, P. Karwat, K. Roszkowska-Purska, M. Gumowska, J. Litniewski, Monitoring breast cancer response to neoadjuvant chemotherapy with ultrasound signal statistics and integrated backscatter, *PLoS ONE* 14 (3) (2019) 1–15, <http://dx.doi.org/10.1371/journal.pone.0213749>.
- [16] L. Sannachi, M. Gangeh, H. Tadayyon, S. Gandhi, F.C. Wright, E. Slodkowska, B. Curpen, A. Sadeghi-Naini, W. Tran, G.J. Czarnota, Breast cancer treatment response monitoring using quantitative ultrasound and texture analysis: comparative analysis of analytical models, *Transl. Oncol.* 12 (10) (2019) 1271–1281, <http://dx.doi.org/10.1016/j.tranon.2019.06.004>.
- [17] M. Byra, K. Dobruch-Sobczak, Z. Klimonda, H. Piotrkowska-Wróblewska, J. Litniewski, Early prediction of response to neoadjuvant chemotherapy in breast cancer sonography using Siamese convolutional neural networks, *IEEE J. Biomed. Health Inform.* (2020) <http://dx.doi.org/10.1109/jbhi.2020.3008040>.
- [18] L. Sheng-Chieh, L. You-Chen, F. Weng-Song, W. Jia-Ming, C. Tzong-Jer, A novel medical image quality index, *J. Digit. Imaging* 24 (5) (2011) 874–882, <http://dx.doi.org/10.1007/s10278-010-9353-y>.
- [19] S. Içer, A. Coskun, T. İkizceli, Quantitative grading using grey relational analysis on ultrasonographic images of a Fatty Liver, *J. Med. Syst.* 36 (4) (2011) 2521–2528, <http://dx.doi.org/10.1007/s10916-011-9724-z>.
- [20] E.B. Mendelson, M. Böhm-Vélez, W.A. Berg, et al., *ACR BI-rads® ultrasound, in: ACR BI-RADS® Atlas, Breast Imaging Reporting and Data System, American College of Radiology, Reston, VA, 2013.*
- [21] K.N. Ogston, I.D. Miller, S. Payne, A.W. Hutcheon, T.K. Sarkar, I. Smith, A. Schofield, S.D. Heys, A new histological grading system to assess response of breast cancers to primary chemotherapy: prognostic significance and survival, *Breast* 12 (5) (2003) 320–327, [http://dx.doi.org/10.1016/S0960-9776\(03\)00106-1](http://dx.doi.org/10.1016/S0960-9776(03)00106-1).
- [22] C.P. Loizou, C.S. Pattichis, *Despeckle Filtering Algorithms and Software for Ultrasound Imaging*, Morgan & Claypool, 2008, <http://dx.doi.org/10.2200/S00116ED1V01Y200805ASE001>.
- [23] J.L. Deng, *Introduction to grey system theory*, *J. Grey Syst.* 1 (1) (1989) 1–24.
- [24] Z. Wang, A.C. Bovik, A universal image quality index, *IEEE Signal Process. Lett.* 9 (3) (2002) 81–84, <http://dx.doi.org/10.1109/97.995823>.
- [25] Z. Wang, A.C. Bovik, H.R. Sheikh, E.P. Simoncelli, Image quality assessment: from error visibility to structural similarity, *IEEE Trans. Image Process.* 13 (4) (2004) 600–612, <http://dx.doi.org/10.1109/TIP.2003.819861>.
- [26] M.L. Oelze, *Quantitative Ultrasound in Soft Tissues: Statistics of Scatterer Property Estimates*, Springer, Dordrecht, 2013, http://dx.doi.org/10.1007/978-94-007-6952-6_3.
- [27] M.I. Daoud, T.M. Bdair, M. Al-Najar, R. Alazrai, A fusion-based approach for breast ultrasound image classification using multiple-ROI texture and morphological analyses, *Comput. Math. Methods Med.* (2016) <http://dx.doi.org/10.1155/2016/6740956>, 2016.
- [28] M.L. Marinovich, N. Houssami, P. Macaskill, F. Sardanelli, L. Irwig, E.P. Mamounas, et al., Meta-analysis of magnetic resonance imaging in detecting residual breast cancer after Neoadjuvant therapy, *JNCI: J. Natl. Cancer Inst.* 105 (5) (2013) 321–333, <http://dx.doi.org/10.1093/jnci/djs528>.
- [29] W.J. Youden, Index for rating diagnostic tests, *Cancer* 3 (1) (1950) 32–35, [http://dx.doi.org/10.1002/1097-0142\(1950\)3:1<32::AID-CNCR2820030106>3.0.CO;2-3](http://dx.doi.org/10.1002/1097-0142(1950)3:1<32::AID-CNCR2820030106>3.0.CO;2-3).
- [30] H. Tadayyon, L. Sannachi, M. Gangeh, et al., A priori prediction of neoadjuvant chemotherapy response and survival in breast cancer patients using quantitative ultrasound, *Sci. Rep.* 7 (45733) (2017) <http://dx.doi.org/10.1038/srep45733>.
- [31] Z. Klimonda, P. Karwat, K. Dobruch-Sobczak, et al., Breast-lesions characterization using quantitative ultrasound features of peritumoral tissue, *Sci. Rep.* 9 (2019) 7963, <http://dx.doi.org/10.1038/s41598-019-44376-z>.
- [32] J. Fernandes, L. Sannachi, W.T. Tran, A. Koven, E. Watkins, F. Hadizad, et al., Monitoring breast cancer response to neoadjuvant chemotherapy using ultrasound strain elastography, *Transl. Oncol.* 12 (2019) 1177–1184, <http://dx.doi.org/10.1016/j.tranon.2019.05.004>.

- [33] H. Cui, D. Zhao, P. Han, X. Zhang, W. Fan, X. Zuo, et al., Predicting pathological complete response after neoadjuvant chemotherapy in advanced breast cancer by ultrasound and clinicopathological features using a nomogram, *Front. Oncol.* 11 (2021) 1–12, <http://dx.doi.org/10.3389/fonc.2021.718531>.
- [34] Y. Huang, J. Le, A. Miao, W. Zhi, F. Wang, Y. Chen, et al., Prediction of treatment responses to neoadjuvant chemotherapy in breast cancer using contrast-enhanced ultrasound, *Gland Surg.* 10 (2021) 1280–1290, <http://dx.doi.org/10.21037/gs-20-836>.
- [35] J. Gu, T. Tong, C. He, M. Xu, X. Yang, J. Tian, et al., Deep learning radiomics of ultrasonography can predict response to neoadjuvant chemotherapy in breast cancer at an early stage of treatment: a prospective study, *Eur. Radiol.* 32 (2022) 2099–2109, <http://dx.doi.org/10.1007/s00330-021-08293-y>.
- [36] K. Dobruch-Sobczak, H. Piotrkowska-Wróblewska, Z. Klimonda, P. Karwat, K. Roszkowska-Purska, P. Clauser, et al., Multiparametric ultrasound examination for response assessment in breast cancer patients undergoing neoadjuvant therapy, *Sci. Rep.* 11 (2021) 1–9, <http://dx.doi.org/10.1038/s41598-021-82141-3>.